UNIVERSITY OF CALIFORNIA SAN DIEGO

Molecular and Cellular Mechanisms for Ionic, Acid-Base, and Ammonia Regulation in Gill Ionocytes of Rockfish and White Sea Bass

A Thesis submitted in partial satisfaction of the requirements
for the degree Master of Science

in

Marine Biology

by

Ryan Jeffrey Myers

Committee in charge:

Martin Tresguerres, Chair
Paul Ponganis
Jennifer Taylor

2023

The Thesis of Ryan Jeffrey Myers is approved, and it is acceptable in quality and form for publication on microfilm and electronically.

University of California San Diego

2023

DEDICATION

I'd like to dedicate this thesis to all those who have helped me along my journey to writing it. Additionally, I would like to single out several individuals who deserve special recognition for their contributions. First, to my parents Kerry and Jeff Myers, thank you for endless support and unconditional love. You have taught me to pursue my passions and encouraged me to find perseverance when my confidence wavered. I am grateful for everything you do and have done for me. Second, to my sister Rachel Myers, thank you for always being a great friend and source of strength. You have provided much laughter and joy to my life. Third, to all the members of the Tresguerres lab who have offered guidance, support, and friendship through my time working here. You all have been essential to my development as a scientist, and I thank you. To my advisor, Dr. Martin Tresguerres, thank you for your patience and guidance. You have challenged me to think critically and push myself academically, making me a better scientist and a better person. To Dr. Alexander Clifford, thank you for mentoring me upon my entering the lab as an undergraduate volunteer. You taught me that science is not linear, and that mistakes and setbacks are an essential part of learning. Finally, Dr. Jennifer Taylor and Dr. Paul Ponganis, thank you for serving on my thesis committee, providing support for my work, and aiding me in my research goals.

EPIGRAPH

"Nothing in this world can take the place of persistence.
Talent will not: nothing is more common than unsuccessful men with talent.
Genius will not; unrewarded genius is almost a proverb.
Education will not: the world is full of educated derelicts.
Persistence and determination alone are omnipotent.
The slogan "Press On" has solved and will always solve the problems of the human race."
-Calvin Coolidge

"I have not failed. I've successfully discovered 10,000 things that won't work."
-Thomas Edison

"The sea, once it casts its spell, holds one in its net of wonder forever."
-Jacques Yves Cousteau

"Time is money, and I have neither."
-Dr. Garfield Kwan

TABLE OF CONTENTS

LIST OF FIGURES

LIST OF ABBREVIATIONS

AMT	Ammonia transporter
ATP	Adenosine triphosphate
BHH	Bromhexine hydrochloride
CAII	Carbonic anhydrase II
cAMP	Cyclic adenosine monophosphate
CFTR	Cystic fibrosis transmembrane conductance regulator
CO_2	Carbon dioxide
DAPI	4′,6-diamidino-2-phenylindole
DTT	Dithiothreitol
EDTA	Ethylenediamine tetra-acetic acid
FISH	Fluorescent *in situ* hybridization
G2A	G2 accumulation; G protein-coupled receptor 132
GAM	Goat anti-mouse
GAR	Goat anti-rabbit
GPCR	G protein-coupled receptor
GPR4	G protein-coupled receptor 4
H^+	Proton/hydrogen ion/acid molecule
H_2O	Water
HCO_3^-	Bicarbonate
HR	H^+-ATPase rich
HRP	Horseradish peroxidase

IHC	Immunohistochemistry
ISHCR	*In situ* hybridization chain reaction
kDA	Kilodalton
KLH	Keyhole limpet hemocyanin
LPC	Lysophosphatidylcholine
NaCl	Sodium chloride
NBC1	Na^+-HCO_3^- cotransporter 1
NH_3	Ammonia
NH_4^+	Ammonium
NHE3	Na^+-H^+ antiporter 3
NKA	Na^+/K^+-ATPase
NKCC	Na^+-K^+-Cl^- cotransporter
OGR1	Ovarian cancer G protein-coupled receptor 1; G protein-coupled receptor 68
PBS	Phosphate buffered saline
PBS-tx	PBS with 0.1% Triton-x
PFA	Paraformaldehyde
pKA	The negative base-10 logarithm of the acid dissociation constant
PMSF	Phenylmethylsulfonyl fluoride
PVDF	Polyvinylidene difluoride
Rh	Rhesus channel
sAC	Soluble adenylyl cyclase
SBH	Sodium borohydride
SDS	Sodium dodecyl sulfate

SEM	Scanning electron microscopy
SPC	Sphingosylphosphorylcholine
SSC	Sodium chloride sodium citrate
SSCT	Sodium chloride sodium citrate w/ Tween 20
TBS-T	Tris-buffered saline w/ Tween 20
TDAG8	T cell death-associated gene 8; G protein-coupled receptor 65
TE	Tris-EDTA
tmAC	Transmembrane adenylyl cyclase
TMAO	Trimethylamine N-oxide

ACKNOWLEDGEMENTS

This work was funded by the National Science Foundation (NSF), Biology- Integrative and Organismal Systems #1754994. Project: “Acid/base sensing and regulation of multiple physiological processes in fish” to Professor Martin Tresguerres.

ABSTRACT OF THE THESIS

Molecular and Cellular Mechanisms for Ionic, Acid-Base, and Ammonia Regulation in Gill Ionocytes of Rockfish and White Sea Bass

by

Ryan Jeffrey Myers

Master of Science in Marine Biology

University of California San Diego, 2023

Martin Tresguerres, Chair

Ionocytes are specialized epithelial ion-transporting cells that play major roles in maintaining blood ionic, ammonia, and acid-base homeostasis of internal fluids. In fish, these functions predominantly take place at the gills. While multiple studies have characterized various gill ionocyte types specialized for NaCl, H^+, HCO_3^- or ammonia transport in elasmobranchs and freshwater teleosts, the putative presence of ionocyte types in marine teleosts remains unclear and it is not known whether all of these functions take place within the same cell. Here, I used immunohistochemistry (IHC) to investigate the presence and cellular localization of ionocytes

and various ion-transporting proteins in gills of splitnose rockfish (*Sebastes diploproa*) and white seabass (*Atractoscion nobilis*), two marine teleost species with distinct environmental pressures and behavioral tendencies. Based on high expression of basolateral Na^+/K^+-ATPase (NKA), ionocytes were abundantly present in the gill filament and in the basal region of the lamellae of both rockfish and white seabass. In rockfish, every NKA-rich ionocyte also expressed cystic fibrosis transmembrane conductance regulator (CFTR), Na^+-H^+ antiporter 3 (NHE3), and a Rhesus channel (Rh) in their apical membrane which had the "pit" morphology typical described for marine teleost gill ionocytes. This suggests that rockfish gills have a single ionocyte type that performs NaCl, H^+, and ammonia excretion. The gill NKA-rich ionocytes of white seabass also co-expressed NHE3 in its apical membrane which, interestingly, demonstrated abundant extended microvilli instead of a pit morphology. In addition, CFTR was present in cells that were not NKA-rich, and Rh channel was predominantly present in pavement cells. Finally, I investigated the presence and cellular localization of the G protein-coupled receptor GPR4, which is a sensor of extracellular pH in mammalian kidney cells. GPR4 gene orthologs were detected in gill transcriptomes from both species. In white seabass, *in situ* hybridization chain reaction (ISHCR) showed the presence of GPR4 mRNA in various gill cells including NKA-rich ionocytes. Furthermore, immunohistochemistry revealed localization of the protein on the apical membrane of NKA-rich ionocytes and pavement cells, suggesting a role in sensing pH of the water flowing over the gill epithelium. These findings improve our knowledge about general and species-specific gill cellular mechanisms used by marine teleosts to maintain blood ionic, ammonia, and acid-base homeostasis, which can help identified physiological differences that determine adaptation to different environments and lifestyles as well as responses to varying

environmental conditions resulting from natural variability, anthropogenic impacts, and aquaculture.

INTRODUCTION

Ionocytes are specialized cells that mediate the transport of ions across animal epithelia for diverse physiological functions including blood ionic, osmotic, ammonia and acid-base regulation. In aquatic animals, the majority of these functions are performed by the gills (reviewed in Evans et al., 2005). The gills of freshwater teleost fishes have multiple ionocyte types, each of which contain a specific set of proteins. For example, tilapia gills have at least three ionocyte types (Hiroi et al., 2008), rainbow trout gills have been hinted to have two or three (Brannen and Gilmour, 2018), and zebrafish gills have at least four (Hwang and Chou, 2013). The various ionocyte types are proposed to be differentially activated according to the fish' physiological needs. In contrast, it is generally assumed that the gills of marine teleosts have a single ionocyte type that performs NaCl, H^+, HCO_3^-, and ammonia excretion (Hiroi and MacCormick, 2012). However, the molecular mechanisms in marine teleost gill ionocytes have received much less attention than those of freshwater teleosts.

For teleosts, the ionic and osmotic challenges experienced in seawater are diametrically opposed to those in freshwater. To counteract the osmotic loss of water and the diffusive gain of NaCl, marine teleosts drink seawater, absorb NaCl and water across the intestine, and actively excrete the excess NaCl across the gills (Smith, 1930). The gill ionocytes that excrete NaCl express abundant Na^+/K^+-ATPase (NKA) in their basolateral membrane, which energize transcellular Cl^- excretion through basolateral $Na^+/K^+/2Cl^-$ cotransporters (NKCC, slc12a2) and apical Cl^- channels called cystic fibrosis transmembrane conductance regulator (CFTR, ABC35). The resulting transepithelial potential drives paracellular Na^+ excretion (Silva et al., 1977).

Marine teleosts fish gills also excrete H^+ for blood acid-base regulation. In the few marine species that it has been investigated, [rainbow trout, blue-throated wrasse (*Oncorhynchus mykiss*, *Pseudolabrus tetrious*, Edwards, 1999), Mozambique tilapia (*Oreochromis mossambicus*, Inokuchi et al., 2008), and European sea bass (*Dicentrarchus labrax*, Montgomery et al., 2022)] this process seems to take place in the same NKA-rich ionocytes that excrete NaCl. The low intracellular Na^+ concertation generated by NKA coupled with the high Na^+ concentration in seawater drive the excretion of H^+ in exchange for Na^+ *via* apical Na^+/H^+ exchanger 3 (NHE3, slc9a3).

Fish gills also excrete ammonia waste. Because ammonia is constantly being produced by protein catabolism, its total concentration in the bloodstream is generally higher than that in the water. However, ammonia speciates NH_4^+ ion and NH_3 gas and with pKa~ 9.3, and the higher pH of seawater compared to that of fish internal fluids implies NH_3 diffusion back into the animal. Some animals prevent this by utilizing acid-trapping of NH_3 as NH_4^+ at the apical surface (reviewed in Tresguerres et al., 2020), vigorous stirring of the apical boundary layer to transport NH_3 away from the epithelium (Thomsen et al., 2016), or active NH_4^+ excretion *via* apical NHEs (Clifford et al., 2022) or ammonia transporters (AMTs). Despite being a gas, NH_3 is a polar molecule and thus its diffusion across cellular membranes is facilitated by Rhesus (Rh) channels (Reviewed in Weiner and Verlander, 2017). Evidence for Rhs in NKA-rich ionocytes and pavement cells of pufferfish (*Takifugu rubripes*) gill suggests that they may be involved in NH_3 excretion in marine teleost fish (Nakada et al., 2007).

These responses to ionic challenges show that marine teleosts utilize ionocytes for NaCl, H^+, and nitrogenous waste, but it remains unclear if these are distinct cell types. This study looks to use the proteins known to be involved in the excretion of these ions to identify if these processes are carried out in multiple ionocyte types.

In addition to identifying ionocyte types in marine teleosts, this study looks to identify the sensor relevant to initiating H^+ excretion in response to blood acidosis. To effectively regulate the processes relevant to excreting acids and bases, the organism must have a method of sensing when the blood pH has exceeded baseline levels and activate the relevant cellular response. In fish, the specific mechanism for activating H^+ excretion in response to acidosis is unknown. Previous work in elasmobranchs has shown that base excreting ionocytes utilize the cellularly localized bicarbonate sensor soluble adenylyl cyclase (sAC) (Roa & Tresguerres, 2016). This means it is plausible that acid excreting ionocytes may have evolved a similar localized mechanism for acid sensing, however there is currently no data that supports this. Potential localized H^+ sensors can be found in the group of proteins known as G-Protein Coupled Receptors (GPCRs).

GPCRs are a large class of proteins known to act as sensing mechanisms involved in many physiological processes and signaling chains. They are membrane bound receptors with 7 transmembrane domains that are associated with guanine nucleotide-binding proteins (G proteins) which send signals received by the GPCR using various secondary signaling molecules. GPCRs are known to be involved in taste, smell, hormone regulation, neurotransmission, and some are sensitive to H^+ (Reviewed by Hill, 2006).

Four GPCRs are known to be H^+ sensitive; GPR4, OGR1, TDAG8, and G2A. They share conserved regions with histidine residues which are the H^+ binding sites (Justus et al., 2013). H^+-sensitive GPCRs can be coupled with the G-protein Gs, which when bound to transmembrane Adenylyl Cyclases (tmACs), triggers the tmAC to produce the secondary messaging molecule cyclic adenosine monophosphate (cAMP). cAMP is a secondary messenger that can activate a wide variety of pathways used in the regulation of cellular processes including protein kinase A (PKA) phosphorylation, exchange protein activated by cAMP (EPAC), and cyclic nucleotide-activated channels (CNAC)(Reviewed in Tresguerres et al., 2019).

Of the four acid sensitive GPCRs, GPR4, OGR1, and G2A have homologs in teleost fish (Mochimaru et al., 2015; Ichijo et al., 2016). GPR4 and OGR1 are the most likely candidates as G2A has the lowest sensitivity to H^+ of the four proteins and there is data suggesting it may bind with other substrates such as small lipid molecules lysophosphatidylcholine (LPC), sphingosylphosphorylcholine (SPC) (Radu et al., 2005). In mouse kidney, GPR4 is an essential sensor involved in concentrating acid in the urine (Sun et al., 2010). The kidney's role in acid excretion in mammals is similar to the gills role in acid excretion in fish, making it possible that the acid sensing mechanism is evolutionarily conserved. GPR4 would need to be basolaterally located to effectively sense blood pH. I hypothesize that GPR4 is the H^+ receptor responsible for triggering the signaling pathway to initiate the cell's response to acidosis.

Finally, this study looks to investigate how ionocyte distribution and composition differs in species with distinct metabolic strategies and environmental challenges. Two local examples are splitnose rockfish (*Sebastes diploproa*) and white seabass (*Atractoscion nobilis*).

Splitnose rockfish are found in the kelp forest and around rocky seafloors off the eastern Pacific coast from Baja California to the Gulf of Alaska. They are generally lethargic, utilizing camouflage and physical factors in the environment, such as rocks or kelp, to stay hidden. Juveniles tend to be found at a depth of ~0-20 m, with a trend of moving deeper as they age, with adults being found as deep as 795 m (Boehlert, 1997). In the shallow waters (7-17 m) of the kelp forest, pH and pCO_2 are highly variable with pH ranging from ~7.7 to ~8.2 and $pCO2$ ranging from ~250 to ~1000 μatm (Frieder et al., 2012). At depths of ~200 m, pH can be as low as 7.5 (Nam et al., 2011). Rockfish living in these environments would be continuously exposed to these conditions which suggests they may have a high tolerance for CO_2 and pH fluctuations.

In contrast, white seabass are highly mobile fish that occupy the coastal open ocean. They travel in schools and are known to cover large distances, with instances of tagged white seabass traveling 555 kilometers over an 80-day period, or about 8 kilometers a day (Aalbers and Sepulveda, 2015). Along with their long-distance traveling, they are known to be elusive prey and adept predators, utilizing bursts of speed to cover short distances quickly. They are found at depths of 0-122 meters (Thomas, 1968). Off the coast of Southern California, surface waters have a pCO_2 of ~400 and a pH of ~8.0 (Sutton et al., 2021). In the open ocean, these parameters tend to have less variation than in the kelp forest, making the environmental conditions faced by white seabass more stable than those faced by splitnose rockfish. The differences between behavioral strategies and environmental pressures of white seabass and splitnose rockfish make them an interesting comparison when investigating how these factors affect the physiological strategies utilized by marine fish.

Overfishing, pollution, and climate change have caused fish populations to decline in recent years. Due to this decline, it is vitally important that conservation efforts recognize the physiological differences between species to take effective action for protecting each population. In addition, it is important for scientists to understand variances in the tolerance of at-risk species as some will be better adapted to endure the increasing CO_2 concentrations associated with climate change.

METHODS

Study Animals

Animal care and experimental procedures were approved by the SIO-UCSD animal care committee under the Institutional Animal Care and Use Committee protocol (#S10320). White seabass were supplied as larvae by Hubbs SeaWorld Research Institute's hatchery facility located in Carlsbad, California. Splitnose rockfish were caught from kelp paddies offshore of La Jolla. Both species were raised in the Hubbs Experimental Aquarium at Scripps Institution of Oceanography at the University of California San Diego. The aquarium used flowthrough seawater sourced from La Jolla Shores. Water temperature was ~15˚C and dissolved oxygen was ~90%. Splitnose rockfish were fed daily to satiation with 2.5 mm classic fry pellets from Skretting and white seabass were fed twice weekly to satiation with 8.0 mm trout pellets from Skretting (Skretting, 2023). Photoperiod was 12h light:12h dark.

Gill Tissue Collection

Fish were euthanized by overdose of tricaine methanesulfonate (0.5 g/L). Average total length and mass of sampled splitnose rockfish was ~12 cm and ~30 g. Average total length and mass of sampled white seabass was ~45 cm and ~ 600 g. Gills were dissected, filaments were removed from the arch and stored in RNA later for transcriptome construction, immediately flash frozen in liquid nitrogen for Western blotting, or placed in ice-cold fixative solution [4% paraformaldehyde (PFA) in phosphate buffered saline (PBS), pH 7.8] for immunohistochemistry

(IHC) and *in situ* hybridization chain reaction (ISHCR). After 12 h fixation, gill samples were stored in 70% ethanol at 4˚C.

Transcriptomics

50 mg of splitnose rockfish and white seabass gill tissue sample were transferred into 1 mL of TRIzol reagent (Thermo Fisher 15596026) and were homogenized on ice with a handheld motorized mortar and pestle (Kimble Kontes, Düsseldorf, Germany). Crude homogenates were centrifuged at 1,000g for 1 min and the supernatant was collected. RNA was extracted in RNA spin columns (RNAEasy Mini; Qiagen, Hilden, Germany) and treated with DNAse I (ezDNase; ThermoFisher, 11766051) to remove traces of genomic DNA. RNA quantity was determined by spectrophotometry (Nanodrop2000; Thermo Fisher) and RNA integrity was determined with an Agilent 2100 Bioanalyzer (Agilent; Santa Clara, CA). Poly-A enriched complementary DNA (cDNA) libraries were constructed using the TruSeq RNA Sample Preparation Kit (Illumina; San Diego, CA). mRNA was selected against total RNA using oligo(dt) magnetic beads and the retained RNA was chemically sheared into short fragments in a fragmentation buffer, followed by first- and second-strand cDNA synthesis using random hexamer primers. Illumina adaptor primers (Forward P5-Adaptor, 50AATGAT-ACGGCGACCACCGAGA30; Reverse P7-Adaptor 50-CGTAT-GCCGTCTTCTGCTTG-30) were then ligated to the synthesized fragments and subjected to end-repair processing. After agarose gel electrophoresis, 200–300 bp insert fragments were selected and used as templates for downstream PCR amplification and cDNA

library preparation. The samples (1 mg RNA) were sent for RNAseq Poly-A sequencing with the Illumina NovoSeq 6000 platform (Novogene; Beijing, China).

Upon receiving the transcriptome sequences, known nucleotide sequences for each protein of interest were gathered from species with close genetic relation to splitnose rockfish and white seabass using the online resource available from the National Center for Biotechnology Information (NCBI). 10-15 closely related sequences were selected to create hidden Markov models that would be searched against the transcriptome using the program HMMER (HMMER, 2023). HMMER identified the sequence or sequences of highest similarity, indicating it was likely a coding sequence for the protein of interest. Once identified, the sequence would be used to design probes for ISHCR or to confirm specificity with epitopes of primary antibodies to be used for Western blotting or IHC.

Antibodies

Mouse monoclonal anti-NKA antibody α-5 was purchased from the Developmental Studies Hybridoma Bank (Iowa City, IA, USA). This antibody was raised against the α subunit of chicken NKA and universally and specifically detects NKA from vertebrates including agnathans, elasmobranchs, and teleosts (Kwan et al., 2019, Roa et al., 2014; Clifford et al., 2022).

The antibodies against the other proteins were all polyclonal and raised in rabbit. Antibodies against CFTR were purchased from Alomone Labs (Jerusalem, Israel) and recognize the peptide

KEETEEEVQDTRL within human CFTR, which is 75% identical (9/12) and 92% similar (11/12) to CFTR from splitnose rockfish and white sea bass (Figure 1a).

Antibodies against NHE3 were a kind donation by Dr. Junya Hiroi (St Marianna University School of Medicine, Kawaski, Japan). These antibodies were raised against two peptides within rainbow trout (*Oncorhynchus mykiss*) NHE3 (GDEDFEFSEGDSASG and PSQRAQLRLPWTPSNLRRLAPL). They specifically recognize NHE3 in a variety of teleost fishes including alewife (*Alosa pseudoharengus*, Christensen et al., 2012), Japanese eel (*Anguilla japonica*, Seo et al., 2013), Common Carp (*Cyprinus carpio*, Wright et al., 2016), and European sea bass (*Dicentrarchus labrax*; Montgomery et al., 2022). Both epitopes are highly conserved in NHE3 from splitnose rockfish and 100% conserved in NHE3 from white sea bass (Figure 1b,c).

Antibodies against Rhcg were a generous gift from Dr. Susan Edwards (Appalachian State University, NC, USA). These antibodies were raised against the peptide CYEDRAYWEVPEEEVTY within hagfish Rhcg (*Eptatretus stoutii*, Edwards et al., 2015; Clifford et al., 2022), which is 56% identical (9/16) and 69% similar (11/16) to Rhcg from splitnose rockfish and white sea bass (Figure 1d).

Antibodies against GPR4 were purchased from Alomone Labs (Jerusalem, Israel). They recognize the peptide RDRYNHTFSFEKFPME within rat GPR4, which is 69% identical (11/16) and 94% similar (15/16) to GPR4 from splitnose rockfish and white seabass (Figure 1e).

The secondary antibodies for Western blot included goat anti-mouse IgG-HRP and goat anti-rabbit IgG-HRP conjugate (Bio-Rad, Hercules, CA, USA). The secondary antibodies for IHC

included goat anti-mouse Alexa Fluor 488 and goat anti-rabbit Alexa Fluor 647 (Invitrogen, Grand Island, USA).

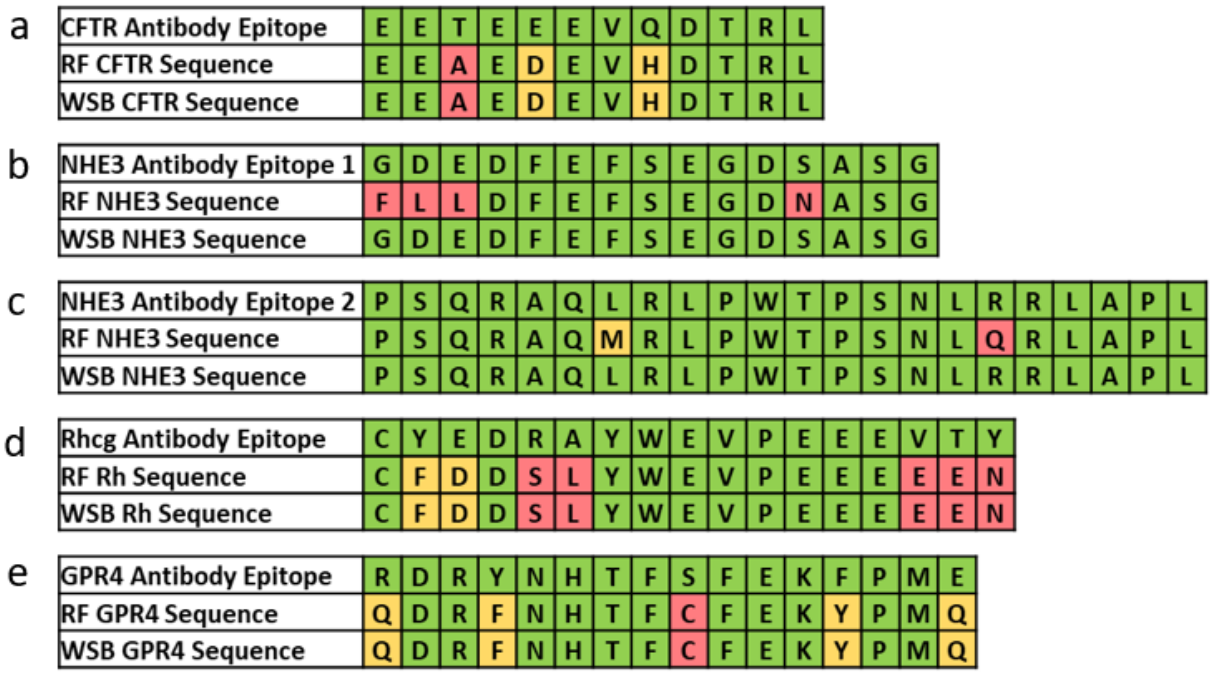

Figure 1. Epitope alignments in splitnose rockfish and white seabass for CFTR (a), NHE3 (b,c), Rhcg (d), and GPR4 (e).

Western Blotting

Frozen gills were homogenized on ice with a handheld motorized mortar and pestle (Kimble Kontes, Düsseldorf, Germany) in homogenization buffer (1mg:10µl) containing a protease inhibitor cocktail (250 mM sucrose, 1 mM EDTA, 30 mM Tris, 10 mM bromhexine hydrochloride (BHH), 200 mM phenylmethylsulfonyl fluoride (PMSF), mM dithiothreitol (DTT), pH 7.5). The resulting mixture was centrifuged at 500g for 10 min at 4˚C. The pellet

containing large debris was discarded; a portion of the supernatant was saved ("crude homogenate") and the rest was further centrifuged at 21,000g for 1 h at 4˚C. The supernatant was saved as the "cytosolic fraction" and the pellet was resuspended in ~50-80µl homogenization buffer, matching the supernatant volume removed, as the "membrane fraction". Total protein concentration in all fractions was determined using the Bradford assay (Bradford, 1976). Samples were combined with an equal volume of Laemmli Sample Buffer (BioRad, Laboratories, Inc., Hercules, CA, USA) containing 10% 2-mercaptoethanol and heated at 70˚C for 10 min. 20µg total protein/lane was loaded into a 10% sodium dodecyl sulfate (SDS) gel and run at 200V for 45 min at room temperature. Proteins were then transferred to a polyvinylidene difluoride (PVDF) membrane using a wet transfer cell (BioRad) filled with Towbin buffer (25 mM Tris, 192 mM glycine, pH 8.3, 20% methanol) for 16 h at 4˚C. PVDF membranes were then blocked in tris-saline buffer (137mM NaCl, 3mM KCl, 19mM Tris base, pH7.4) with 0.1% Tween 20 (TBS-T) and 10% nonfat dry milk (blocking buffer) for 1 h at room temperature. The PVDF membrane was incubated in the selected primary antibody, diluted 1:2,000 for NKA and 1:1,000 for CFTR, NHE3, Rhcg, and GPR4 in blocking buffer for 16 h at 4˚C. Following the primary antibody incubation, the membrane was washed in TBS-T 3 times, 5 min each, and incubated with the HRP-linked secondary antibodies (1:5,000 in blocking buffer) for 1 h at room temperature. The membrane was then washed as described above prior to revealing the bands through addition of ECL Prime Western Blotting Detection Reagent (GE Healthcare, Waukesha, WI) imaging on a ChemiDocTM MP system (BioRad).

Immunohistochemistry

Fixed gill samples that had been stored in 70% ethanol were rehydrated in PBS containing 0.1% Triton-x (PBS-Tx) and washed 3 times, 15 min each. To quench autofluorescence, samples were washed in PBS with 1mg/mL sodium borohydride (SBH) 6 times, 10 min each, at 4˚C (Kwan et al., 2022). Samples were then washed in PBS-Tx 3 times, 15 min each at room temperature and incubated with blocking buffer (2% normal goat serum and 0.02% keyhole limpet hemocyanin in PBS) for 1 h at room temperature. After blocking, samples were incubated in 1:250 primary antibody (1:500 for anti-NKA) in PBS for 16 h at 4˚C. Samples were then washed in PBS-Tx 3 times, 15 min each and incubated in 1:1,000 secondary antibody with 1:2,000 4′,6-diamidino-2-phenylindole (DAPI) nuclear stain in PBS for 1 h at room temperature. Finally, samples were washed in PBS-Tx 3 times, 15 min each. Samples were immersed in PBS, mounted onto a depressed glass slide fitted with a glass cover slip and imaged using a Zeiss LSM800 inverted confocal microscope equipped with a Zeiss LD LCI Plan Apochromat 40x/1.2 lmm Korr DIC M27 objective and Zeiss ZEN 2.6 blue edition software (Cambridge, United Kingdom).

***In situ* Hybridization Probes**

Split-initiator probes for *in situ* hybridization chain reaction (ISHCR) were designed against white seabass GPR4 mRNA using probemaker 3.0 from the Ozpolat lab (insitu_probe_generator, 2021). Probe sets were created by the probemaker program and BLAST searched against the white seabass transcriptome to confirm specificity. Probes were purchased

from Integrated DNA Technologies (IDT) (oPools product; idtdna, 2023). Probes were resuspended in TE buffer (10mM Tris, 1mM ethylenediamine tetra-acetic acid (EDTA), pH 8.0) and frozen at -20˚C for storage.

Hairpins for ISHCR were generously donated by Dr. Amro Hamdoun (Scripps Institution of Oceanography, University of California San Diego, La Jolla, CA, USA). They were purchased from Molecular Instruments with B2 initiator and 647 fluorophore specifications (molecularinstruments, 2023).

In Situ Hybridization Chain Reaction with Immunohistochemistry

Fixed white seabass gill samples that had been stored in 70% ethanol were rehydrated in PBS-Tx 3 times, 15 min each at room temperature. Samples were then permeabilized in a detergent solution [1.0% SDS, 0.5% Tween 20, 50.0mM Tris-HCl (pH 7.5), 1.0mM EDTA (pH 8.0), 150.0mM NaCl, in molecular grade water] 2 times, 30 min each at room temperature. Following permeabilization, samples were equilibrated in hybridization buffer [30% formamide, 5x sodium chloride sodium citrate (5x SSC; 750mM NaCl, 75mM sodium citrate), 9mM citric acid (pH 6.0), 0.1% Tween 20, 50µg/mL heparin, 1x Denhardt's solution (0.02% Ficoll 400, 0.02% polyvinylpyrrolidone, and 0.02% bovine serum albumin), 10% dextran sulfate, in molecular grade water] for 30 min at 37˚C. During sample equilibration, probes were added to hybridization buffer to create a 18nM probe solution and prewarmed to 37˚C. Samples were then incubated in probe solution for 16 h at 37˚C. Following hybridization, samples were washed in probe wash buffer (30% formamide, 5X sodium chloride sodium citrate (SSC), 9mM citric acid

(pH 6.0), 0.1% Tween 20, 50µg/mL heparin, in molecular grade water) 4 times, 15 min each at 37˚C. Samples were then washed in SSCT (SSC and 0.1% Tween 20) 2 times, 5 min each at room temperature. Samples were equilibrated to amplification buffer (SSCT and 10% dextran sulfate) for 30 min at room temperature. During sample equilibration, the hairpins were added to amplification buffer to create a 60nM solution, linearized by heating to 95˚C for 90 sec then cooled to room temperature for 30 min. Samples were then incubated in prepared hairpin solution for 16 h at room temperature. Following amplification, gills were washed in SSCT 5 times with washes 1, 2 and 5 lasting 5 min and washes 3 and 4 lasting 30 min.

RESULTS

NKA Protein Expression in Splitnose Rockfish and White Seabass

Western blotting confirmed the specificity of the anti-NKA antibody in splitnose rockfish and white seabass. The crude homogenate and membrane fraction of homogenized gill tissue produced bands at 100 kDa in both species (Figure 2). This is consistent with the predicted size for the NKA protein, which indicates the anti-NKA antibody specifically recognizes NKA.

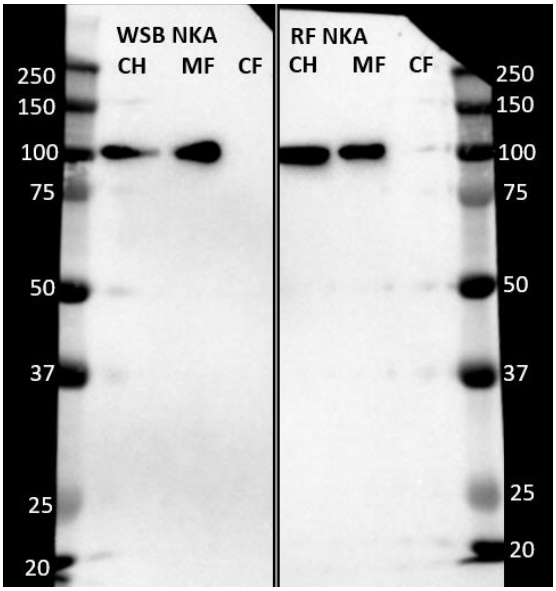

Figure 2. Western blot detection of NKA in splitnose rockfish and white seabass. The anti-NKA antibody was used and detects a ~100kDa protein which matches the predicted size of the NKA protein. The blot was run with crude homogenate (CH), membrane fraction (MF), and cytosolic fraction (CF) from both species. Precision Plus Dual Color Protein Standards (BioRad) were used to determine protein molecular weights.

Western blots using the anti-CFTR, anti-NHE3, anti-Rhcg, and anti-GPR4 antibodies to confirm the specificity of the antibodies were attempted, but no protein bands were produced. Possibilities for the lack of bands are discussed in the appendix.

Comparison of Ionocyte Localization in Splitnose Rockfish and White Seabass

IHC with the anti-NKA antibody identified the NKA-rich ionocytes in the gills of splitnose rockfish and white seabass (Figure 3). In both species, the ionocytes are concentrated on the trailing edge of the lamellae. Both gills have ordered and consistent ionocytes for ~5-7 cells along the trailing edge. The number of cells in this area is consistent for both species, however the splitnose rockfish gill lamellae have less length, meaning that relative to the white seabass gill, more length of the lamellae is covered by the ionocytes. Unlike splitnose rockfish, the white seabass gill has individual ionocytes extending further away from the trailing edge along the length of the lamellae. In addition, the white seabass gill displayed a higher density of filamentous ionocytes than the splitnose rockfish gill.

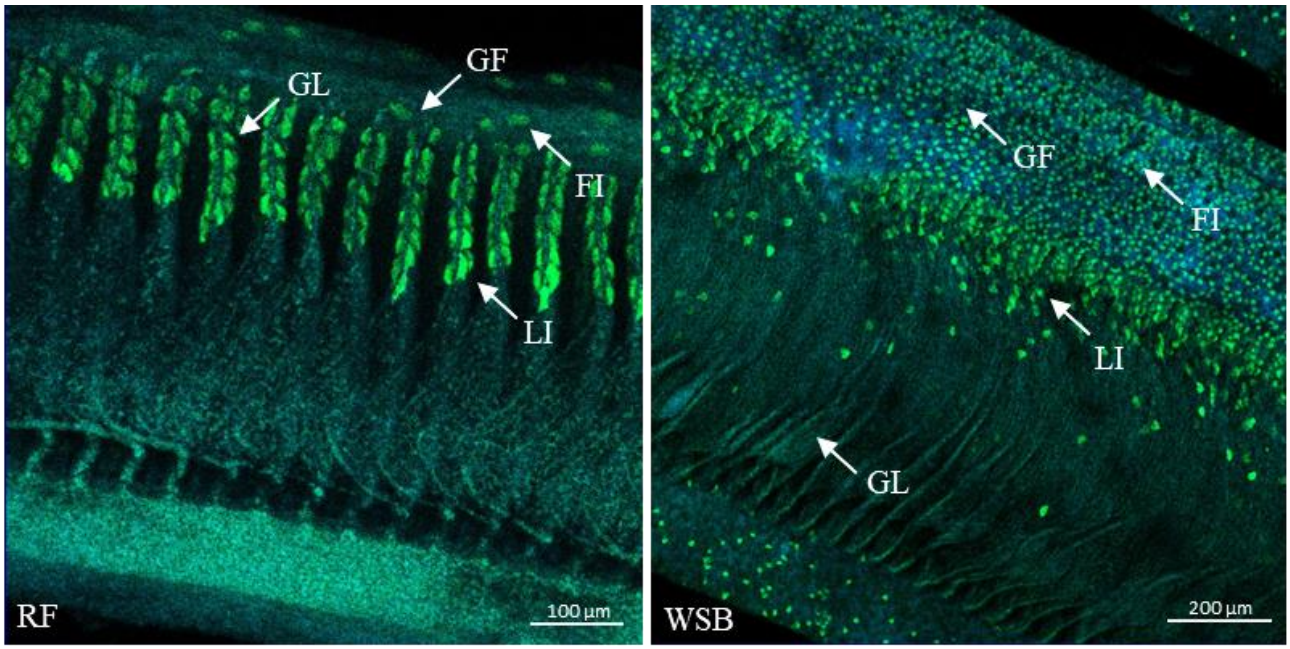

Figure 3. Immunohistochemistry with the anti-NKA antibody (green) in splitnose rockfish and white seabass. Arrows identify gill filament (GF), gill lamellae (GL), filamentous NKA-rich ionocytes (FI) and lamellar NKA-rich ionocytes (LI).

Subcellular Localization of CFTR, NHE3, and Rh

In the splitnose rockfish gill, IHC with the anti-CFTR antibody (red) showed clear apical staining throughout the sample and was consistently present in every NKA-rich ionocyte, both filamentous and lamellar (Figure 4a-c). The fluorescence pattern shows a clear apical pit that is distinct from the basolateral fluorescence from the anti-NKA antibody (green). This is consistent with what is known about CFTR localization in other teleost gills.

In the white seabass gill, fluorescence from the anti-CFTR antibody was not colocalized with NKA-rich ionocytes (Figure 4d-f). Interestingly, there is signal from cells that are not NKA-rich ionocytes. The signal is present throughout the entire membrane of these cells. Comparison with no-primary negative controls confirms that this signal is not autofluorescence. In addition, there is the presence of points of high signal intensity throughout the sample. These high intensity spots were also present in the no-primary negative control white seabass gill and are background signal.

Figure 4. Immunohistochemistry with the anti-CFTR (red) and anti-NKA (green) antibodies in splitnose rockfish and white seabass. Lamellae and filament of splitnose rockfish gill (A) shows apical CFTR in every NKA-rich ionocyte. Single cell images of filamentous (B) and lamellar (C) ionocytes. Lamellae and filament of white seabass gill (D) shows CFTR signal from some cell membranes. Single cell image of a lamellar cell with this signal (E). Arrows identify the apical pit (AP) CFTR signal in splitnose rockfish and membrane signal (MS) in white seabass.

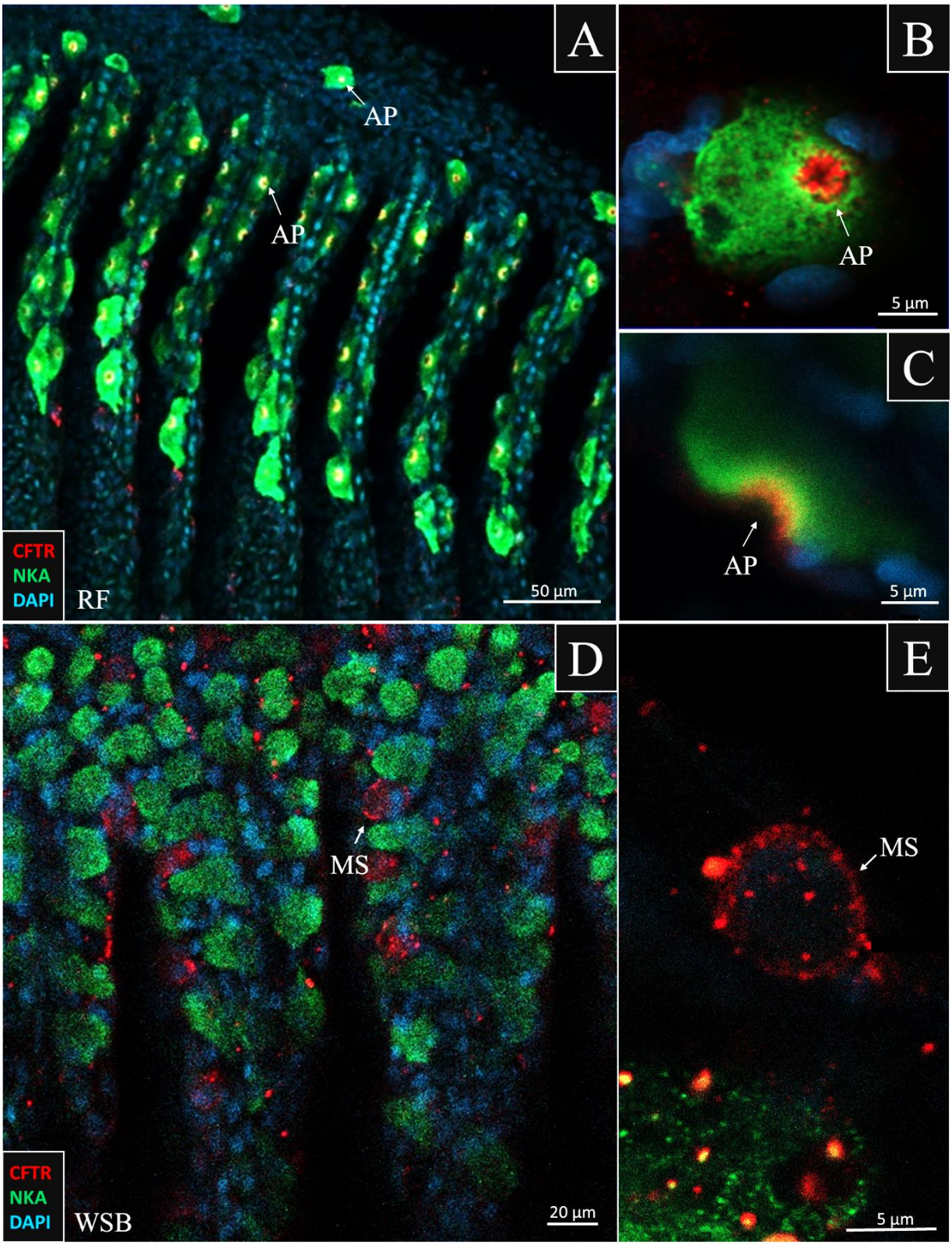
A
AP
AP
CFTR
NKA
DAPI
RF
50 µm
B
AP
5 µm
C
AP
5 µm
D
MS
CFTR
NKA
DAPI
WSB
20 µm
E
MS
5 µm

IHC with the anti-NHE3 antibody (red) showed clear apical staining in both the splitnose rockfish and white seabass gills (Figure 5), which is consistent with what is known about NHE3 localization in other teleost gills. The signal was present throughout the sample in every NKA-rich ionocyte, both filamentous and lamellar. In the splitnose rockfish gill, the NHE3 signal shows a clear apical pit while the NKA signal (green) shows the staining of the basolateral membrane (Figure 5b-c). Comparison with no-primary negative controls confirms that this signal is not autofluorescence.

In the white seabass gill, the NHE3 signal is apical, but lamellar ionocytes have apical microvillae extension while filamentous ionocytes had an apical pit (Figure 5D-F). Comparison with no-primary negative controls confirms that this signal is not autofluorescence. In addition, there is the presence of points of high signal intensity throughout the sample. These high intensity spots were also present in the no-primary negative control white seabass gill and are background signal.

Figure 5. Immunohistochemistry with the anti-NHE3 (red) and anti-NKA (green) antibodies in splitnose rockfish and white seabass. Lamellae and filament of splitnose rockfish (A) and white seabass (D) gills show apical NHE3 in every NKA-rich ionocyte. Single cell images of filamentous (B,E) and lamellar (C,F) ionocytes. Orthogonal projection of filamentous ionocyte to show apical pit (E). Arrows identify the apical pit (AP) and apical signal (AS) NHE3 signal.

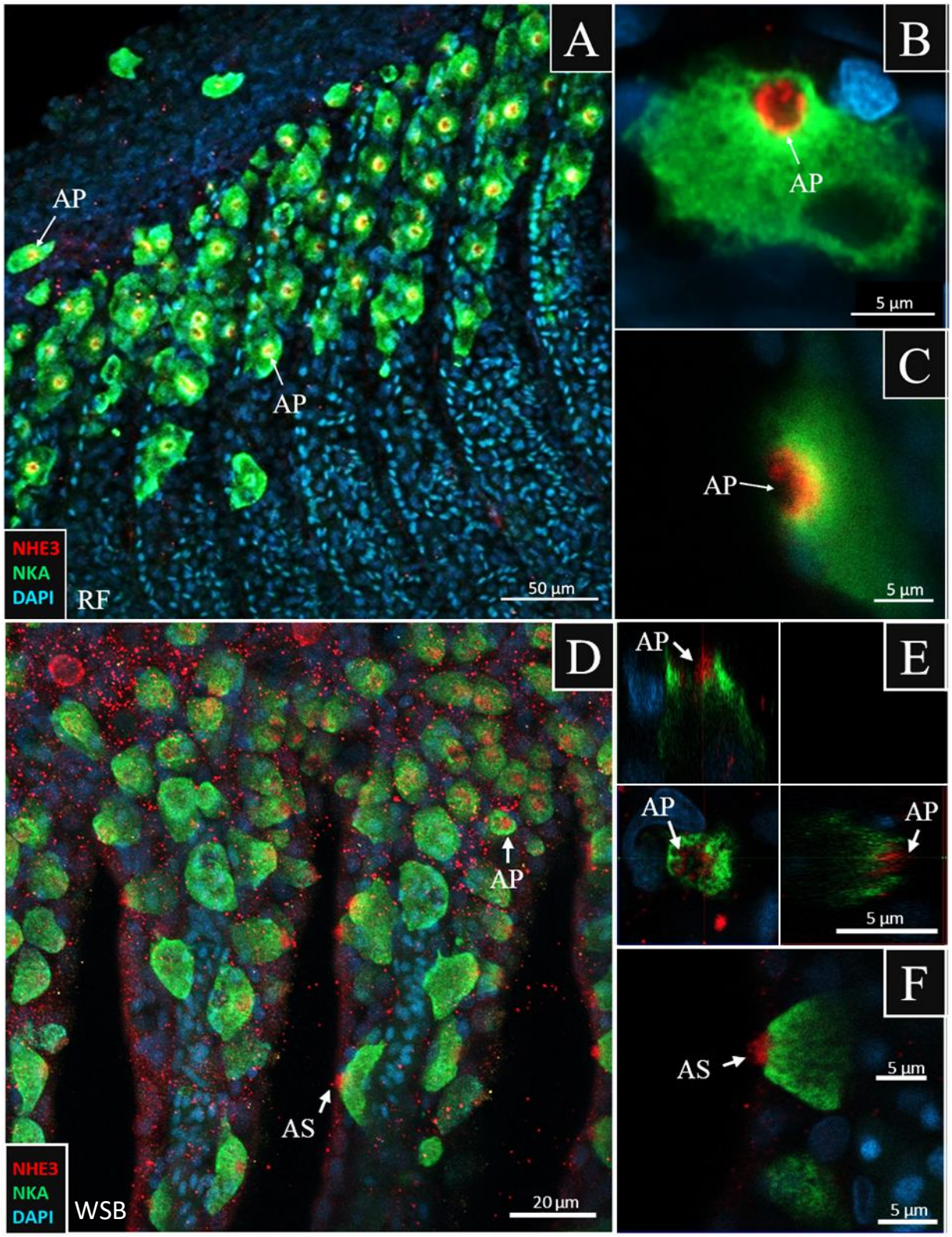
A
AP
AP
NHE3
NKA
DAPI
RF
50 µm
B
AP
5 µm
C
AP
5 µm
D
AP
AS
NHE3
NKA
DAPI
WSB
20 µm
E
AP
AP
AP
5 µm
F
AS
5 µm
5 µm

In the splitnose rockfish gill, IHC with the anti-Rhcg antibody (red) showed clear apical staining throughout the sample and was consistently present in every NKA-rich ionocyte, both filamentous and lamellar (Figure 6a-c). As mentioned in the methods section, our transcriptomic analysis was unable to differentiate Rhbg and Rhcg sequences in both splitnose rockfish and white seabass. The construction of a phylogenetic tree of Rh sequences would be required to properly place the sequence results that were found. Consequently, we will be referring to the signal as Rh signal and will not specify the specific Rh channel. The fluorescence pattern shows a clear apical pit that is distinct from the basolateral fluorescence from the anti-NKA antibody (green).

In the white seabass gill, there is no apical signal from the anti-Rhcg antibody in NKA-rich cells, however there is signal on the membrane of pavement cells on the lamellae. Comparison with no-primary negative controls confirms that this signal is not autofluorescence. In addition, there is the presence of points of high signal intensity throughout the sample. These high intensity spots were also present in the no-primary negative control white seabass gill and are background signal.

Figure 6. Immunohistochemistry with the anti-Rhcg (red) and anti-NKA (green) antibodies in splitnose rockfish and white seabass. Lamellae and filament of splitnose rockfish gill (A) shows apical Rh in every NKA-rich ionocyte. Single cell images of filamentous (B) and lamellar (C) ionocytes. Lamellae of white seabass gill (D) shows Rh signal from the membrane of pavement cells. Image of lamellar pavement cells with this signal (E). Arrows identify the apical pit (AP) Rh signal in splitnose rockfish and pavement cell membrane signal (PCMS) in white seabass.

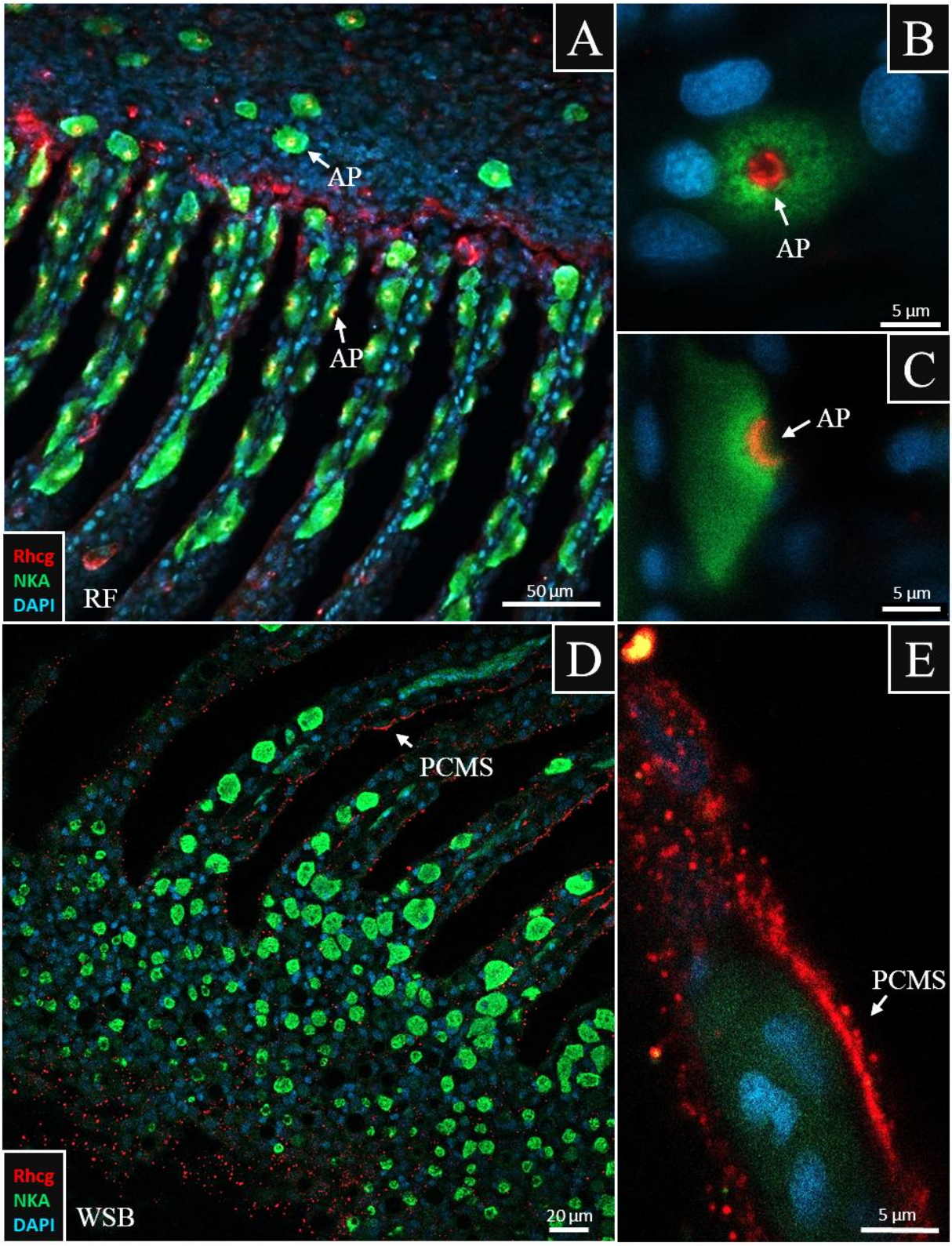
A
AP
AP
Rhcg
NKA
DAPI
RF
50 µm
B
AP
5 µm
C
AP
5 µm
D
PCMS
Rhcg
NKA
DAPI
WSB
20 µm
E
PCMS
5 µm

GPR4 in White Seabass

ISCHR with GPR4 probes (red) in white seabass gill showed cells which contained expression of GPR4 mRNA (Figure 7a). Cells with both NKA protein and GPR4 mRNA were present when ISHCR was used in conjunction with IHC using the anti-NKA antibody (green) (Figure 7b). GPR4 signal was not present in all NKA-rich ionocytes. Comparison with no-probe negative controls confirmed that the signal is not autofluorescence. The signal from the GPR4 probe in filamentous ionocytes was more distinct than that of lamellar ionocytes.

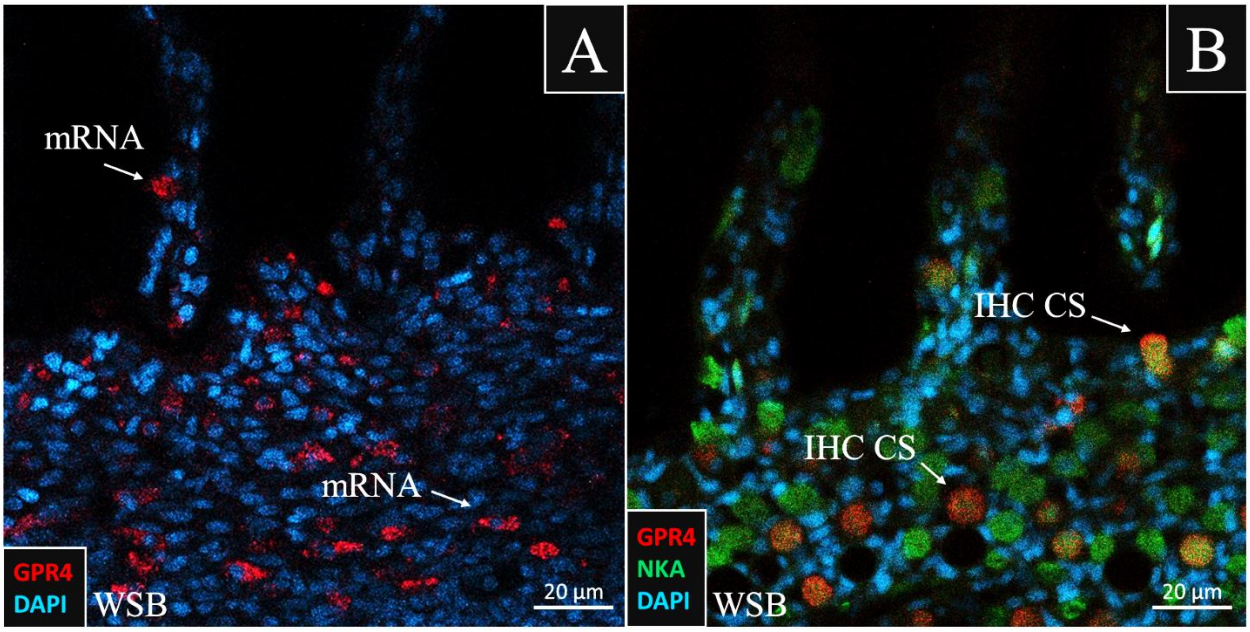

Figure 7. ISHCR with the GPR4 probe (red) in white seabass gill (A). ISHCR with the GPR4 probe (red) and anti-NKA (green) antibody in white seabass gill (B). Arrows identify the GPR4 mRNA signal (mRNA) and costaining with NKA antibody (IHC CS).

IHC with the anti-GPR4 antibody (red) in white seabass gill showed apical staining with a clear apical pit (Figure 8). This provides data on the localization of the GPR4 protein that was not available with the ISHCR technique. Staining from the GPR4 antibody was also present in the membrane of pavement cells surrounding the NKA-rich ionocytes. Comparison with no-primary negative controls confirmed the signal is not autofluorescence.

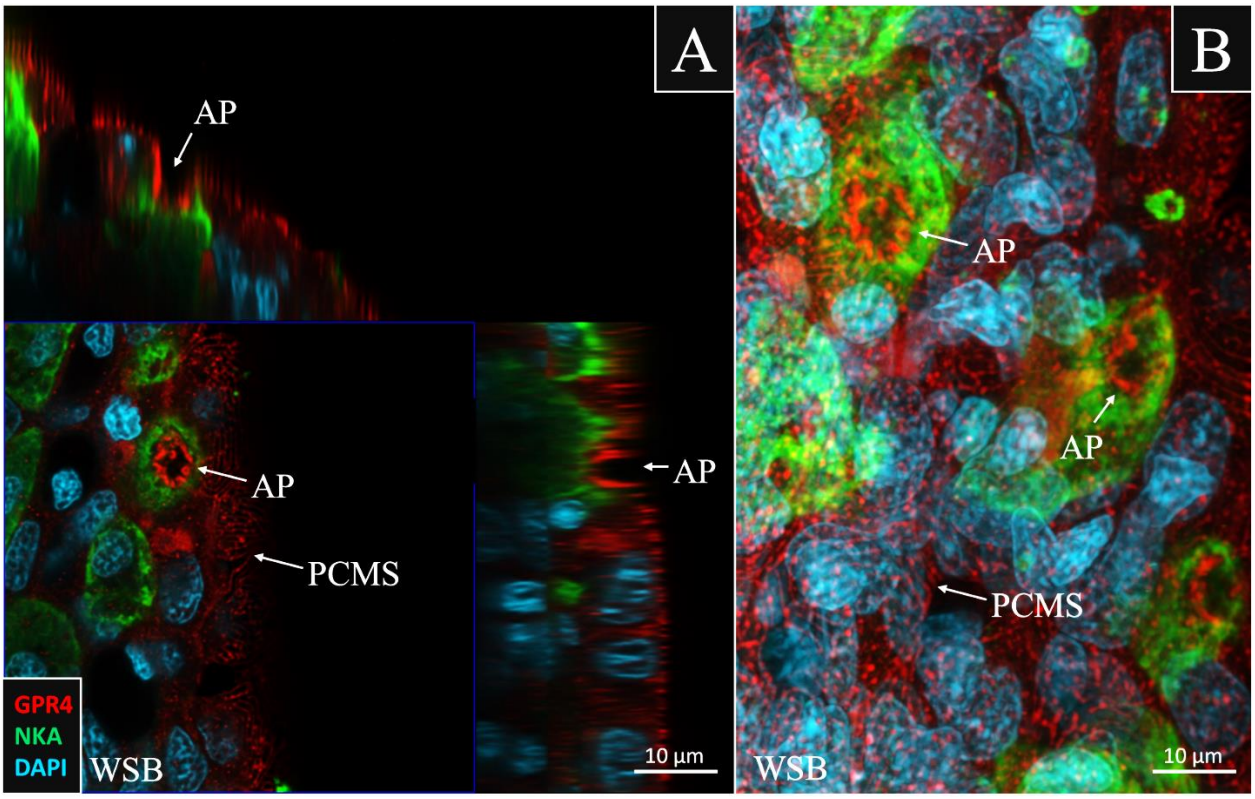

Figure 8. Immunohistochemistry with the anti-GPR4 (red) and anti-NKA (green) antibodies in white seabass. Orthogonal projection created from z-stack of a filamentous ionocyte (A) shows apical staining of GPR4. Maximum intensity projection of this z-stack (B). Arrows identify the apical pit (AP) GPR4 signal and pavement cell membrane signal (PCMS).

DISCUSSION

Ionocyte Localization in Splitnose Rockfish and White Seabass

The distribution of NKA-rich ionocytes in splitnose rockfish and white seabass were compared to look for potential differences in ionocyte quantity or area of lamellae covered. Due to their differences in behavioral tendencies and environmental stressors, the two species may require different capacities for ion excretion, in particular H^+ excretion capacities. Rockfish are exposed to high environmental pCO_2, leading to higher blood pCO_2 and respiratory blood acidosis, which is counteracted by increased H^+ excretion. In their environment, white seabass likely experience fewer respiratory blood acidoses, however they likely experience more frequent metabolic acidoses, due to their active behavior. We were interested in how these dynamics may affect the distribution and quantity of ionocytes.

The two species showed few differences in the quantity of ionocytes on each lamellae, however the white seabass gill is larger so the lamellar area covered by ionocytes is relatively less than in the splitnose rockfish. This difference in lamellar length is likely due to the difference in length and weight of the fish sampled. Total lamellar area, including lamellar length, tends to increase with fish weight (Muir, 1969). In addition, total lamellar area increases with total fish length in orange spotted grouper (*Epinephelus coioides*, Mohammed, 2018). Considering these factors, it is unsurprising that the white seabass lamellae are longer than the splitnose rockfish.

All NKA-Rich Cells May Have the Capacity for NaCl, H^+ and NH_4^+ Excretion in Splitnose Rockfish

Apical localization of CFTR, NHE3, and Rh in NKA-rich ionocytes is not a novel finding in teleost fish as all three transport proteins have been identified on the apical membrane of other species, however it is significant that each protein was found in all NKA-rich ionocytes in splitnose rockfish. This suggests that in splitnose rockfish, all NKA-rich ionocytes have the capacity to play a role in NaCl, H^+, and NH_3/NH_4^+ excretion. This is similar to HR cells in zebrafish which also transport NaCl, H^+ and NH_3/NH_4^+ (Reviewed in Hwang et al., 2011). The colocalization of NHE3 and Rh may aid in the excretion of nitrogenous waste as H^+ excreted by NHE3 can combine with NH_3 transported by Rh, leading to formation of NH_4^+ and maintaining a lower pNH_3 in the boundary layer, providing continued NH_3 diffusion. Acid trapping of NH_3 is utilized by freshwater fish (Reviewed in Ip and Chew, 2010), however, it may be less advantageous in marine teleosts as seawater has a higher buffering capacity than freshwater and requires more H^+ to be excreted to achieve significant acidification. Splitnose rockfish are not a highly mobile species, limiting the mixing of seawater around their gills, which may allow them to create an acidic microenvironment in the apical pit of ionocytes. In addition, NKA-rich ionocytes containing all 3 discussed mechanisms of ion transport, as opposed to having 3 specialized subtypes, may allow for a higher capacity of ion regulation as each NKA-rich ionocyte can be involved in excretion of a particular ion in events of acute concentration increases.

The type of Rh seen on the apical pit of splitnose rockfish ionocytes was unable to be identified through our transcriptomic analysis. Previous work in teleost gills has shown an Rhcg ortholog, Rhcg1, in the apical membrane of NKA-rich ionocytes while Rhbg is in the basolateral membrane of pavement cells (Nakada et al., 2007), suggesting the antibody may be specific to Rhcg, however additional analyses will be required (see Further Experiments).

Localization of CFTR, NHE3, and Rh in White Seabass

In white seabass, the CFTR signal was not found in the apical membrane of NKA-rich cells, however it was found in the membrane of other cells in the gill. The signal was seen around the entirety of the membrane. These "CFTR-rich" cells were layered between NKA-rich ionocytes, appearing in proximity, but distinctly separate, from NKA-rich ionocytes. This is an interesting finding that contrasts the apical pit staining seen in splitnose rockfish. CFTR in the apical pit of gill NKA-rich ionocytes has been cited in multiple seawater acclimated teleosts including killifish (*Fundulus heteroclitus*, Marshall et al., 2002), mudskipper (*Periophthalmodon schlosseri*, Wilson et al., 2000), Hawaiian goby (*Stenogobius hawaiiensis*, McCormick et al., 2003), Plotosidae catfish (*Plotosus lineatus*, Kolbadinezhad et al., 2018) and now splitnose rockfish. The idea that most teleosts primarily use apical CFTR in NKA-rich ionocytes for Cl^- excretion is widely accepted, however some telosts have other mechanisms of NaCl excretion. The euryhaline Plotosidae catfish has an extra-branchial salt secreting dendritic organ, which is suggested to perform most of the NaCl excretion required by the organism, with the gills taking a secondary role (Kolbadinezhad et al., 2018). The lack of apical CFTR in white seabass suggests

they may also have different mechanisms for excreting NaCl. It is also possible that white seabass evolved to use a different chloride transporter such as a different chloride channel, cation-chloride cotransporter (Slc12 family), or anion exchanger (Slc26 family), to excrete Cl^-. This would explain the lack of apical CFTR expression in NKA-rich ionocytes, but not its presence in other gill cells. Finally, CFTR expression could be regulated in white seabass to only appear at specific times, however this is unlikely as NaCl is entering the organism at a consistent rate, so fluctuations in NaCl excretion are not likely required.

NHE3 was found in the apical membrane of white seabass gills, however in lamellar ionocytes, the signal showed apical microvillae extension rather than an apical pit. In European seabass, microvillae extend from the apical pit during H^+ excretion, likely to maximize the surface area for excretion (Montgomery et al., 2022). The microvillae seen in white seabass could also be the result of a blood acidosis event. During the sampling of the white seabass, the fish thrashed and expended energy in response to being caught in the net and transferred to the anesthesia holding tank. It is possible that this response caused a blood acidosis immediately prior to sampling the gills. In contrast, the staining in splitnose rockfish showed a clear apical pit, which is interesting as the same protocol was applied to both species, with splitnose rockfish reacting to being caught in a net and thrashing in a similar fashion. Filamentous ionocytes did show an apical pit, similar to what was seen in the splitnose rockfish gills. This difference in morphology between filamentous and lamellar ionocytes may indicate different functions of these cells, however additional analyses will be required.

Rh signal in white seabass was present in the apical membrane of pavement cells but was not present in the apical membrane of NKA-rich ionocytes. There is evidence of an Rhcg ortholog, Rhcg2 on the apical membrane of pavement cells in pufferfish (Nakada et al., 2007). It is possible that splitnose rockfish only have the Rhcg2 ortholog, which would explain the absence of signal in NKA-rich ionocytes, however, further investigation of the transcriptome is required (see Further Experiments). In contrast to splitnose rockfish, Rh and NHE3 were not colocalized in white seabass. This eliminates the possibility of joint function to acidify a compartment for acid trapping NH_3. White seabass swim continuously, which may cause increased water flow over pavement cells and move excreted NH_3 away from the gill minimizing potential reabsorption.

The differences in CFTR and Rh localization between splitnose rockfish and white seabass is unlikely to be the result of unspecific binding as the epitope alignments of the epitope sites are very similar.

GPR4 in White Seabass

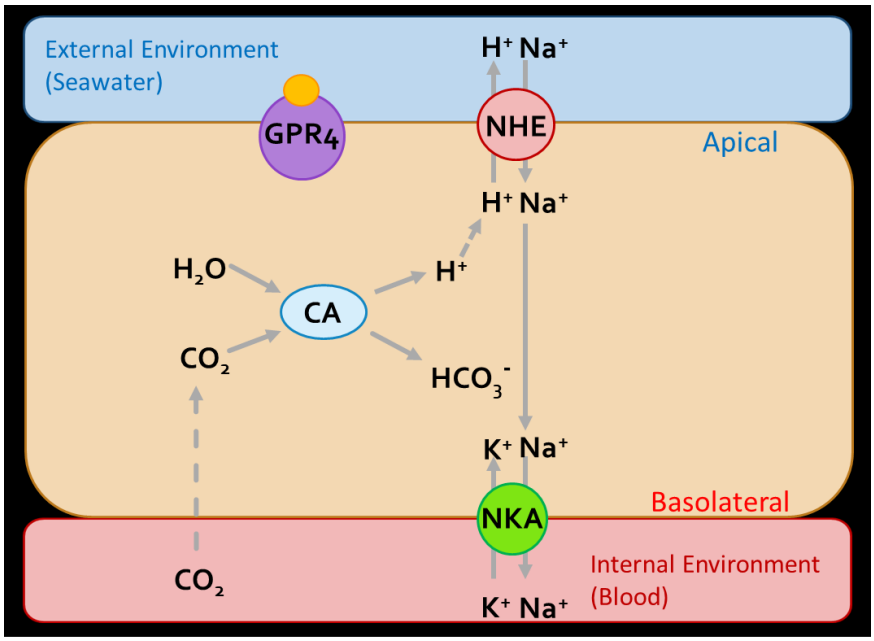

Figure 9. Localization of GPR4 on the apical membrane of the NKA-rich ionocyte. Illustration of how apical GPR4 would be ineffective at sensing the pH of the blood. The process of H^+ excretion is likely initiated by a different sensor.

The localization of GPR4 to the apical membrane was unexpected as contact with the external environment rules it out as a sensor for blood pH. Its function in the apical membrane is unknown, however its presence may mean that it is involved in sensing the pH of the apical pit microenvironment. The lack of GPR4 in the apical membrane indicates that a different sensing mechanism must be responsible for initiating the response to blood acidosis. OGR1 is a possible sensor as it has been identified in teleost gill transcriptomes, but no localization data is present. If OGR1 were to be in the basolateral membrane it may play a role in sensing the blood pH of teleost fish. Remote sensors such as neural or hormonal pathways are also a possibility.

GPR4 signal was seen most distinctly in filament ionocytes, which shows it is colocalized with NHE3 on the apical membrane. Its function can only be speculated as the grouping with tmAC allows for many signaling pathways to be activated, however it may serve as a signal to decrease NHE3 activity if the apical pit becomes too acidic. GPR4 was also seen on the apical membrane of pavement cells, which shows it is colocalized with Rh. In these cells, it may have a role interacting with Rh channels, increasing their activity during periods of high acidity. This would minimize the amount of excreted ammonia that speciates to NH_3, limiting the amount that could potentially be reabsorbed. Further investigation of its function will be necessary to determine its specific role.

CONCLUSION

This thesis shows multiple aspects of the cellular mechanisms used by marine teleosts to maintain blood ionic, ammonia, and acid-base homeostasis while comparing those mechanisms in two species with distinct environmental challenges and behavioral tendencies. CFTR, NHE3, and Rh were shown to be apically colocalized in the gill NKA-rich ionocytes of splitnose rockfish, providing evidence for a single ionocyte type that functions to excrete NaCl, H^+, and NH_3. White seabass were shown to have a different localizations of CFTR and Rh, while NHE3 showed the same localization, but had a different apical morphology in lamellar NKA-rich ionocytes. The different characteristics seen between splitnose rockfish and white seabass highlight how distinct environmental and physiological factors may affect the mechanisms utilized by different species of fish.

Additionally, this thesis shows GPR4 is an external H^+ sensor in the gills of white seabass. The apical localization across filamentous NKA-rich ionocytes and pavement cells displays that it is a sensor for multiple cell types. Further research into its function will be important for determining the mechanism it triggers and what its role is in these cells.

Finally, the comparison of splitnose rockfish and white seabass illustrates the importance of studying many species when thinking about specific mechanisms in physiology. The intricacies between species are easily lost in generalizations. It is important to conservation efforts and the aquaculture industry for these intricacies to be well understood for proper management in response to anthropogenic impacts and aquaculture environments.

APPEDIX

Further Experiments:

Throughout this thesis, there were multiple attempted and proposed experiments that were not able to be completed due to time and resource constraints. The first set of experiments that would supplement the current data well is additional Western blots to validate the specificity of the GAR antibodies. Western blotting with the GAM anti-NKA antibody confirmed the specificity of the antibody to NKA protein. The same protocol was attempted multiple times to obtain results with the anti-CFTR, anti-NHE3, anti-Rhcg, and anti-GPR4 antibodies. Unfortunately, each attempt failed to produce any signal for these antibodies. Application of ponceau S stain to the membrane revealed that protein transferred successfully to the membrane. In addition, successful imaging with the anti-NKA antibody on the same membrane confirmed the imaging system was operational. This led to the belief that the GAR-HRP secondary antibody was not functioning properly and was responsible for the lack of signal. Direct imaging of the GAR-HRP and GAM-HRP secondary antibodies at 1:100 concentration in blocking buffer confirmed that the GAR-HRP was producing less signal in comparison to the GAM-HRP. This led to the conclusion that the GAR-HRP was either contaminated or denatured. Further experiments using fresh GAR-HRP aliquots would allow for the validation of these antibodies, which would strengthen the significance of the IHC results.

Additionally, the ISHCR data presented in this thesis would benefit from additional controls. A no-probe negative control was used to rule out autofluorescence, but we did not use controls to confirm probe specificity. Two additional experiments to confirm probe specificity

are using antisense probes and a positive control probe of a different protein. Antisense probes are useful because they share the same chemical properties as the experimental probe but will not bind to the target site. This allows for the ruling out of any unspecific binding due to the chemical properties alone. A different positive control probe would allow for the confirmation that our methods allow the probe to bind to the intended site. A good positive control for this set of data would be an NKA probe, as the cells with high NKA expression can be clearly defined using the anti-NKA antibody. These additional controls would provide strength to the identification of GPR4 mRNA using ISHCR.

Construction of an Rh phylogenetic tree would be valuable as it would allow for the correct identification of the Rh protein that the antibody recognizes. Being able to identify the specific Rh would allow for the comparison to the localizations of Rhbg, Rhcg1, and Rhcg2 seen in other teleost species.

To further investigate the morphological differences seen between splitnose rockfish and white seabass, an additional method of characterizing the morphology would be required. Two methods that would be appropriate are scanning electron microscopy (SEM) and IHC with other known apical markers.

In Situ Hybridization Chain Reaction

Fluorescent *in situ* hybridization (FISH) is a method for fluorescently tagging RNA or DNA in a tissue or cell of interest. The first use of fluorophores linked to complementary RNA was used to label DNA of *Drosophila melanogaster* in 1977 (Rudkin and Stollar, 1977). This led

to an explosion of studies utilizing this technique to visualize the localization of genes in chromosomes and RNA in cells. Although FISH is an excellent tool, the length of traditional FISH probes (500-1,500 bases) restricts its ability to differentiate closely related sequences. This limitation can be addressed by using a cocktail of shorter oligonucleotide probes that span the length of the target sequence (Femino et al., 1998). However, this method can be quite costly as each oligonucleotide requires its own fluorophore. In addition, FISH can damage tissue samples from the high temperature required for hybridization. The melting temperature (T_m) varies depending on the properties of the probe, but long probes generally require higher temperatures of greater than 55˚C with smaller oligos requiring lower temperatures of 37˚C (Reviewed in Young et al., 2020). Although FISH remains a viable option for many studies, these factors must be considered adding difficulty to experimental design in some cases.

The most recent evolution of mRNA detection in tissues builds on the foundation of FISH while minimizing some of its drawbacks. *In situ* hybridization chain reaction (ISHCR) utilizes short probes (25-100 bases) that hybridize with target mRNA sequences while a secondary pair of fluorophore-conjugated sequences known as hairpins initiate a chain reaction (Figure 10). The hairpins (H1 and H2) are designed with sequences that are complementary to one another and allow them to hybridize. The H1 hairpin contains a, b, c, and b′ domains, which are complementary to the a′, b′, c′, and b domains of H2. First, the probe hybridizes with the target mRNA sequence. The probe contains an "a′" initiator sequence that does not hybridize with the rest of the nucleic acids and is designed to recognize the "a" domain of the H1 haripin. This connection provides the base of the chain reaction. The H2 hairpin then recognizes and binds with the complementary domains of the H1 hairpin. The H2 domain ends with an "a" domain

which serves as a "toehold" for another H1 hairpin to bind, which leaves an "a′" domain for the next H2 hairpin. This chain reaction can happen up to 200 times (Tsuneoka and Funato 2020). Each of the hairpins is conjugated with a fluorophore, providing significantly increased signal for each hybridized probe (Choi et al., 2010).

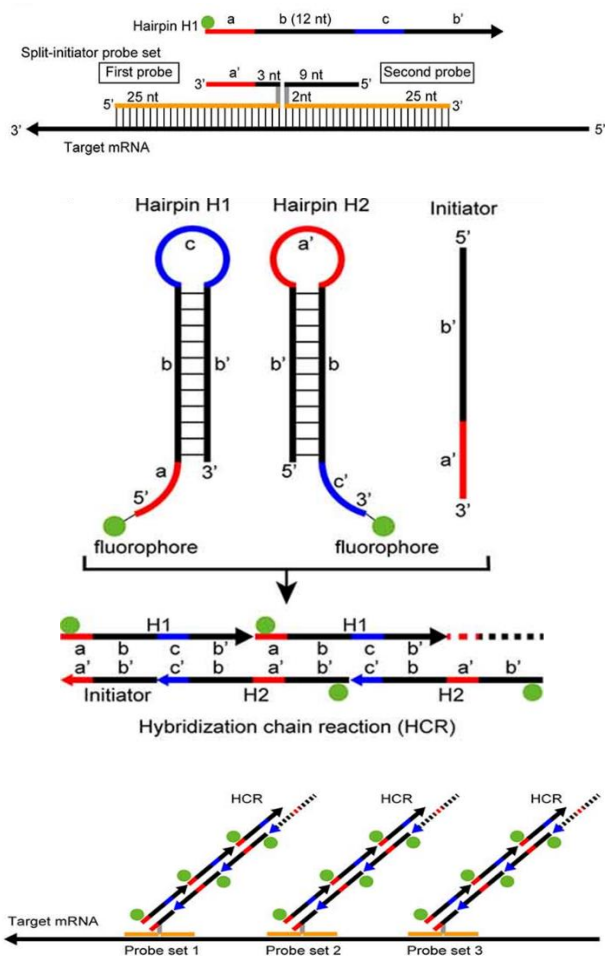

Figure 10. ISHCR diagram (Adapted from Tsuneoka and Funato 2020) Illustration of ISCHR mechanisms including split-initiator probe binding, hairpin specificity, and chain reaction.

ISHCR has numerous advantages over traditional FISH. The amplification step caused by the hairpin chain reaction provides much greater signal to background ratio, which is especially

advantageous when targeting mRNA that has low expression. The shorter probe allows for differentiating between highly similar targets, resulting in increased specificity. In addition, two probes can be used to target one mRNA sequence using a split-initiator probe design (Choi et al., 2018). The split-initiator probe requires both halves of the probe to be present before the chain reaction can occur. This provides additional increases specificity as this blocks the chain reaction from beginning unless the initiator sequences are aligned, which removes the possibility of unbound probe remaining in the sample from starting the reaction. A fourth advantage is that the shorter probes can be hybridized at 37˚C and the amplification reaction takes place at room temperature, which limits damage to tissues.

Finally, the cost of these experiments is reduced if a scientist plans to investigate multiple targets. Traditionally, probes with conjugated fluorophores would need to be designed for each individual target. ISHCR allows for the design of many probes at a low cost, as they lack fluorophores, and every probe can be designed with the same initiator sequence, allowing the same hairpins to recognize each probe used. These factors allow ISHCR to be revolutionary in molecular biology and will unlock *in situ* hybridization as a potential method for many researchers.

REFERENCES

Aalbers, S. A., & Sepulveda, C. A. (2014). Seasonal movement patterns and temperature profiles of adult white seabass (Atractoscion nobilis) off California. Fishery Bulletin, 113(1), 1–14. https://doi.org/10.7755/FB.113.1.1

Blondeau-Bidet, E., Hiroi, J., & Lorin-Nebel, C. (2019). Ion uptake pathways in European sea bass Dicentrarchus labrax. Gene, 692, 126–137. https://doi.org/10.1016/j.gene.2019.01.006

Boehlert, G. W. (1977). Timing of the surface-to-benthic migration in juvenile rockfish, Sebastes diploproa, off southern California | Scientific Publications Office. Fishery Bulletin/US Dept of Commerce National Oceanic and Atmospheric Administration, 75(4). https://spo.nmfs.noaa.gov/content/timing-surface-benthic-migration-juvenile-rockfish-sebastes-diploproa-southern-california

Bradford, M. M. (1976). A rapid and sensitive method for the quantitation of microgram quantities of protein utilizing the principle of protein-dye binding. Analytical Biochemistry, 72, 248–254. https://doi.org/10.1006/abio.1976.9999

Brannen, M., & Gilmour, K. M. (2018). Carbonic anhydrase expression in the branchial ionocytes of rainbow trout. The Journal of Experimental Biology, 221(Pt 5), jeb164582. https://doi.org/10.1242/jeb.164582

Brauner, C. J., Shartau, R. B., Damsgaard, C., Esbaugh, A. J., Wilson, R. W., & Grosell, M. (2019). 3 - Acid-base physiology and CO2 homeostasis: Regulation and compensation in response to elevated environmental CO2. In M. Grosell, P. L. Munday, A. P. Farrell, & C. J. Brauner (Eds.), Fish Physiology (Vol. 37, pp. 69–132). Academic Press. https://doi.org/10.1016/bs.fp.2019.08.003

Choi, H. M. T., Chang, J. Y., Trinh, L. A., Padilla, J. E., Fraser, S. E., & Pierce, N. A. (2010). Programmable in situ amplification for multiplexed imaging of mRNA expression. Nature Biotechnology, 28(11), 1208–1212. https://doi.org/10.1038/nbt.1692

Choi, H. M. T., Schwarzkopf, M., Fornace, M. E., Acharya, A., Artavanis, G., Stegmaier, J., Cunha, A., & Pierce, N. A. (2018). Third-generation in situ hybridization chain reaction: Multiplexed, quantitative, sensitive, versatile, robust. Development (Cambridge, England), 145(12), dev165753. https://doi.org/10.1242/dev.165753

Christensen, A. K., Hiroi, J., Schultz, E. T., & McCormick, S. D. (2012). Branchial ionocyte organization and ion-transport protein expression in juvenile alewives acclimated to freshwater or seawater. Journal of Experimental Biology, 215(4), 642–652. https://doi.org/10.1242/jeb.063057

Claiborne, J. B., Edwards, S. L., & Morrison-Shetlar, A. I. (2002). Acid–base regulation in fishes: Cellular and molecular mechanisms. Journal of Experimental Zoology, 293(3), 302–319. https://doi.org/10.1002/jez.10125

Clifford, A. M., Weinrauch, A. M., Edwards, S. L., Wilkie, M. P., & Goss, G. G. (2017). Flexible ammonia handling strategies using both cutaneous and branchial epithelia in the highly ammonia-tolerant Pacific hagfish. American Journal of Physiology-Regulatory, Integrative and Comparative Physiology, 313(2), R78–R90. https://doi.org/10.1152/ajpregu.00351.2016

Clifford, A. M., Wilkie, M. P., Edwards, S. L., Tresguerres, M., & Goss, G. G. (2022). Dining on the dead in the deep: Active NH4+ excretion via Na+/H+(NH4+) exchange in the highly ammonia tolerant Pacific hagfish, Eptatretus stoutii. Acta Physiologica, 236(2), e13845. https://doi.org/10.1111/apha.13845

Dymowska, A. K., Hwang, P.-P., & Goss, G. G. (2012). Structure and function of ionocytes in the freshwater fish gill. Respiratory Physiology & Neurobiology, 184(3), 282–292. https://doi.org/10.1016/j.resp.2012.08.025

Edwards, S. L., Arnold, J., Blair, S. D., Pray, M., Bradley, R., Erikson, O., & Walsh, P. J. (2015). Ammonia excretion in the Atlantic hagfish (Myxine glutinosa) and responses of an Rhc glycoprotein. American Journal of Physiology-Regulatory, Integrative and Comparative Physiology, 308(9), R769–R778. https://doi.org/10.1152/ajpregu.00355.2014

Edwards, S. L., Tse, C. M., & Toop, T. (1999). Immunolocalisation of NHE3-like immunoreactivity in the gills of the rainbow trout (Oncorhynchus mykiss) and the blue-throated wrasse (Pseudolabrus tetrious). Journal of Anatomy, 195 (Pt 3)(Pt 3), 465–469. https://doi.org/10.1046/j.1469-7580.1999.19530465.x

Evans, D. H., More, K. J., & Robbins, S. L. (1989). Modes of Ammonia Transport Across the Gill Epithelium of the Marine Teleost Fish Opsanus Beta. Journal of Experimental Biology, 144(1), 339–356. https://doi.org/10.1242/jeb.144.1.339

Evans, D. H., Piermarini, P. M., & Choe, K. P. (2005). The Multifunctional Fish Gill: Dominant Site of Gas Exchange, Osmoregulation, Acid-Base Regulation, and Excretion of Nitrogenous Waste. Physiological Reviews, 85(1), 97–177. https://doi.org/10.1152/physrev.00050.2003

Femino, A. M., Fay, F. S., Fogarty, K., & Singer, R. H. (1998). Visualization of single RNA transcripts in situ. Science (New York, N.Y.), 280(5363), 585–590. https://doi.org/10.1126/science.280.5363.585

Frieder, C. A., Nam, S. H., Martz, T. R., & Levin, L. A. (2012). High temporal and spatial variability of dissolved oxygen and pH in a nearshore California kelp forest. Biogeosciences, 9(10), 3917–3930. https://doi.org/10.5194/bg-9-3917-2012

HCR™ RNA-FISH Bundle. (n.d.). https://store.molecularinstruments.com/new-bundle/rna-fish

Hill, S. J. (2006). G-protein-coupled receptors: Past, present and future. British Journal of Pharmacology, 147(Suppl 1), S27–S37. https://doi.org/10.1038/sj.bjp.0706455

Hiroi, J., & McCormick, S. D. (2012). New insights into gill ionocyte and ion transporter function in euryhaline and diadromous fish. Respiratory Physiology & Neurobiology, 184(3), 257–268. https://doi.org/10.1016/j.resp.2012.07.019

Hiroi, J., Yasumasu, S., McCormick, S. D., Hwang, P.-P., & Kaneko, T. (2008). Evidence for an apical Na–Cl cotransporter involved in ion uptake in a teleost fish. Journal of Experimental Biology, 211(16), 2584–2599. https://doi.org/10.1242/jeb.018663

Hwang, P.-P., & Chou, M.-Y. (2013). Zebrafish as an animal model to study ion homeostasis. Pflügers Archiv - European Journal of Physiology, 465(9), 1233–1247. https://doi.org/10.1007/s00424-013-1269-1

Hwang, P.-P., Lee, T.-H., & Lin, L.-Y. (2011). Ion regulation in fish gills: Recent progress in the cellular and molecular mechanisms. American Journal of Physiology-Regulatory, Integrative and Comparative Physiology, 301(1), R28–R47. https://doi.org/10.1152/ajpregu.00047.2011

Ichijo, Y., Mochimaru, Y., Azuma, M., Satou, K., Negishi, J., Nakakura, T., Oshima, N., Mogi, C., Sato, K., Matsuda, K., Okajima, F., & Tomura, H. (2016). Two zebrafish G2A homologs activate multiple intracellular signaling pathways in acidic environment. Biochemical and Biophysical Research Communications, 469(1), 81–86. https://doi.org/10.1016/j.bbrc.2015.11.075

IDT oPools Oligo Pools. (n.d.). https://www.idtdna.com/site/order/poolentry/

Inokuchi, M., Hiroi, J., Watanabe, S., Lee, K. M., & Kaneko, T. (2008). Gene expression and morphological localization of NHE3, NCC and NKCC1a in branchial mitochondria-rich cells of Mozambique tilapia (Oreochromis mossambicus) acclimated to a wide range of salinities. Comparative Biochemistry and Physiology. Part A, Molecular & Integrative Physiology, 151(2), 151–158. https://doi.org/10.1016/j.cbpa.2008.06.012

Insitu_probe_generator. (n.d.). https://github.com/rwnull/insitu_probe_generator

Ip, Y. K., & Chew, S. F. (2010). Ammonia production, excretion, toxicity, and defense in fish: A review. Frontiers in Physiology, 1, 134. https://doi.org/10.3389/fphys.2010.00134

Justus, C., Dong, L., & Yang, L. (2013). Acidic tumor microenvironment and pH-sensing G protein-coupled receptors. Frontiers in Physiology, 4. https://www.frontiersin.org/articles/10.3389/fphys.2013.00354

Karnaky, K. J. (1986). Structure and Function of the Chloride Cell of Fundulus heteroclitus and Other Teleosts. American Zoologist, 26(1), 209–224.

Keys, A., & Willmer, E. N. (1932). "Chloride secreting cells" in the gills of fishes, with special reference to the common eel. The Journal of Physiology, 76(3), 368-378.2.

Kwan, G. T., Finnerty, S. H., Wegner, N. C., & Tresguerres, M. (2019). Quantification of Cutaneous Ionocytes in Small Aquatic Organisms. Bio-Protocol, 9(9), e3227. https://doi.org/10.21769/BioProtoc.3227

Kwan, G. T., & Tresguerres, M. (2022). Elucidating the acid-base mechanisms underlying otolith overgrowth in fish exposed to ocean acidification. Science of The Total Environment, 823, 153690. https://doi.org/10.1016/j.scitotenv.2022.153690

Malakpour Kolbadinezhad, S., Coimbra, J., & Wilson, J. M. (2018). Osmoregulation in the Plotosidae Catfish: Role of the Salt Secreting Dendritic Organ. Frontiers in Physiology, 9. https://www.frontiersin.org/articles/10.3389/fphys.2018.00761

Marshall, W. S., Lynch, E. M., & Cozzi, R. R. F. (2002). Redistribution of immunofluorescence of CFTR anion channel and NKCC cotransporter in chloride cells during adaptation of the killifish Fundulus heteroclitus to sea water. The Journal of Experimental Biology, 205(Pt 9), 1265–1273. https://doi.org/10.1242/jeb.205.9.1265

McCormick, S. D., Sundell, K., Björnsson, B. T., Brown, C. L., & Hiroi, J. (2003). Influence of salinity on the localization of Na+/K+-ATPase, Na+/K+/2Cl- cotransporter (NKCC) and CFTR anion channel in chloride cells of the Hawaiian goby (Stenogobius hawaiiensis). The Journal of Experimental Biology, 206(Pt 24), 4575–4583. https://doi.org/10.1242/jeb.00711

Mochimaru, Y., Azuma, M., Oshima, N., Ichijo, Y., Satou, K., Matsuda, K., Asaoka, Y., Nishina, H., Nakakura, T., Mogi, C., Sato, K., Okajima, F., & Tomura, H. (2015). Extracellular acidification activates ovarian cancer G-protein-coupled receptor 1 and GPR4 homologs of zebra fish. Biochemical and Biophysical Research Communications, 457(4), 493–499. https://doi.org/10.1016/j.bbrc.2014.12.105

Mohammed, F. A. (2018). RELATIONSHIP BETWEEN TOTAL LENGTH AND GILL SURFACE AREA IN ORANGE SPOTTED GROUPER, EPINEPHELUS COIOIDES (Hamilton, 1822). IRAQI JOURNAL OF AGRICULTURAL SCIENCES, 49(5). https://doi.org/10.36103/ijas.v49i5.48

Montgomery, D. W., Kwan, G. T., Davison, W. G., Finlay, J., Berry, A., Simpson, S. D., Engelhard, G. H., Birchenough, S. N. R., Tresguerres, M., & Wilson, R. W. (2022). Rapid blood acid–base regulation by European sea bass (Dicentrarchus labrax) in response to sudden exposure to high environmental CO2. The Journal of Experimental Biology, 225(2), jeb242735. https://doi.org/10.1242/jeb.242735

Muir, B. S. (1969). Gill Dimensions as a Function of Fish Size. Journal of the Fisheries Research Board of Canada, 26(1), 165–170. https://doi.org/10.1139/f69-018

Nakada, T., Westhoff, C. M., Kato, A., & Hirose, S. (2007). Ammonia secretion from fish gill depends on a set of Rh glycoproteins. FASEB Journal: Official Publication of the Federation of American Societies for Experimental Biology, 21(4), 1067–1074. https://doi.org/10.1096/fj.06-6834com

Nam, S., Kim, H.-J., & Send, U. (2011). Amplification of hypoxic and acidic events by La Niña conditions on the continental shelf off California. Geophysical Research Letters, 38(22). https://doi.org/10.1029/2011GL049549

Radu, C. G., Nijagal, A., McLaughlin, J., Wang, L., & Witte, O. N. (2005). Differential proton sensitivity of related G protein-coupled receptors T cell death-associated gene 8 and G2A expressed in immune cells. Proceedings of the National Academy of Sciences of the United States of America, 102(5), 1632–1637. https://doi.org/10.1073/pnas.0409415102

Randall, D. J., Wilson, J. M., Peng, K. W., Kok, T. W. K., Kuah, S. S. L., Chew, S. F., Lam, T. J., & Ip, Y. K. (1999). The mudskipper, Periophthalmodon schlosseri, actively transports NH 4 + against a concentration gradient. American Journal of Physiology-Regulatory, Integrative and Comparative Physiology, 277(6), R1562–R1567. https://doi.org/10.1152/ajpregu.1999.277.6.R1562

Roa, J. N., Munévar, C. L., & Tresguerres, M. (2014). Feeding induces translocation of vacuolar proton ATPase and pendrin to the membrane of leopard shark (Triakis semifasciata) mitochondrion-rich gill cells. Comparative Biochemistry and Physiology. Part A, Molecular & Integrative Physiology, 174, 29–37. https://doi.org/10.1016/j.cbpa.2014.04.003

Roa, J. N., & Tresguerres, M. (2016). Soluble adenylyl cyclase is an acid-base sensor in epithelial base-secreting cells. American Journal of Physiology-Cell Physiology, 311(2), C340–C349. https://doi.org/10.1152/ajpcell.00089.2016

Roa, J. N., & Tresguerres, M. (2017). Bicarbonate-sensing soluble adenylyl cyclase is present in the cell cytoplasm and nucleus of multiple shark tissues. Physiological Reports, 5(2), e13090. https://doi.org/10.14814/phy2.13090

Rudkin, G. T., & Stollar, B. D. (1977). High resolution detection of DNA-RNA hybrids in situ by indirect immunofluorescence. Nature, 265(5593), 472–473. https://doi.org/10.1038/265472a0

Seo, M. Y., Mekuchi, M., Teranishi, K., & Kaneko, T. (2013). Expression of ion transporters in gill mitochondrion-rich cells in Japanese eel acclimated to a wide range of environmental salinity. Comparative Biochemistry and Physiology Part A: Molecular & Integrative Physiology, 166(2), 323–332. https://doi.org/10.1016/j.cbpa.2013.07.004

Silva, P., Solomon, R., Spokes, K., & Epstein, F. (1977). Ouabain inhibition of gill Na-K-ATPase: Relationship to active chloride transport. The Journal of Experimental Zoology, 199(3), 419–426. https://doi.org/10.1002/jez.1401990316

Smith, H. W. (1930). The absorption and excretion of water and salts by marine teleosts. American Journal of Physiology-Legacy Content, 93(2), 480–505. https://doi.org/10.1152/ajplegacy.1930.93.2.480

Sun, X., Yang, L. V., Tiegs, B. C., Arend, L. J., McGraw, D. W., Penn, R. B., & Petrovic, S. (2010). Deletion of the pH Sensor GPR4 Decreases Renal Acid Excretion. Journal of the American Society of Nephrology : JASN, 21(10), 1745–1755. https://doi.org/10.1681/ASN.2009050477

Sutton, A. J., Williams, N. L., & Tilbrook, B. (2021). Constraining Southern Ocean CO2 Flux Uncertainty Using Uncrewed Surface Vehicle Observations. Geophysical Research Letters, 48(3), e2020GL091748. https://doi.org/10.1029/2020GL091748

Thomas, J. C. (1968). Fish Bulletin 142. Management of The White Seabass (Cynoscion Nobilis) In California Waters.

Thomsen, J., Himmerkus, N., Holland, N., Sartoris, F. J., Bleich, M., & Tresguerres, M. (2016). Ammonia excretion in mytilid mussels is facilitated by ciliary beating. Journal of Experimental Biology, 219(15), 2300–2310. https://doi.org/10.1242/jeb.139550

Tresguerres, M., Clifford, A. M., Harter, T. S., Roa, J. N., Thies, A. B., Yee, D. P., & Brauner, C. J. (2020). Evolutionary links between intra- and extracellular acid–base regulation in fish and other aquatic animals. Journal of Experimental Zoology Part A: Ecological and Integrative Physiology, 333(6), 449–465. https://doi.org/10.1002/jez.2367

Tresguerres, M., Milsom, W. K., & Perry, S. F. (2019). 2—CO2 and acid-base sensing. In M. Grosell, P. L. Munday, A. P. Farrell, & C. J. Brauner (Eds.), Fish Physiology (Vol. 37, pp. 33–68). Academic Press. https://doi.org/10.1016/bs.fp.2019.07.001

Tsuneoka, Y., & Funato, H. (2020). Modified in situ Hybridization Chain Reaction Using Short Hairpin DNAs. Frontiers in Molecular Neuroscience, 13, 75. https://doi.org/10.3389/fnmol.2020.00075

Weiner, I. D., & Verlander, J. W. (2017). Ammonia Transporters and Their Role in Acid-Base Balance. Physiological Reviews, 97(2), 465–494. https://doi.org/10.1152/physrev.00011.2016

Wilkie, M. P. (2002). Ammonia excretion and urea handling by fish gills: Present understanding and future research challenges. Journal of Experimental Zoology, 293(3), 284–301. https://doi.org/10.1002/jez.10123

Wilson, J. M., Randall, D. J., Donowitz, M., Vogl, A. W., & Ip, A. K. (2000). Immunolocalization of ion-transport proteins to branchial epithelium mitochondria-rich cells in the mudskipper (Periophthalmodon schlosseri). The Journal of Experimental Biology, 203(Pt 15), 2297–2310. https://doi.org/10.1242/jeb.203.15.2297

Wilson, R. W., & Taylor, E. W. (1992). Transbranchial Ammonia Gradients and Acid-Base Responses to High External Ammonia Concentration in Rainbow Trout (Oncorhynchus Mykiss) Acclimated to Different Salinities. Journal of Experimental Biology, 166(1), 95–112. https://doi.org/10.1242/jeb.166.1.95

Wright, P. A., Wood, C. M., Hiroi, J., & Wilson, J. M. (2016). (Uncommon) Mechanisms of Branchial Ammonia Excretion in the Common Carp (Cyprinus carpio) in Response to Environmentally Induced Metabolic Acidosis. Physiological and Biochemical Zoology, 89(1), 26–40. https://doi.org/10.1086/683990

Young, A. P., Jackson, D. J., & Wyeth, R. C. (2020). A technical review and guide to RNA fluorescence in situ hybridization. PeerJ, 8, e8806. https://doi.org/10.7717/peerj.8806